JVSTB
JOURNAL OF VACUUM SCIENCE AND TECHNOLOGY B

Impact of post-growth thermal annealing and environmental exposure on the unintentional doping of CVD graphene films

Hossein Sojoudi, Jose Baltazar, Clifford Henderson, and Samuel Graham

Citation: J. Vac. Sci. Technol. B **30**, 041213 (2012); doi: 10.1116/1.4731472
View online: http://dx.doi.org/10.1116/1.4731472
View Table of Contents: http://avspublications.org/resource/1/JVTBD9/v30/i4
Published by the AVS: Science & Technology of Materials, Interfaces, and Processing

Impact of post-growth thermal annealing and environmental exposure on the unintentional doping of CVD graphene films

Hossein Sojoudi
Electronic Manufacturing and Reliability Laboratory and Woodruff School of Mechanical Engineering, Georgia Institute of Technology, 771 Ferst Drive, Atlanta, Georgia 30332

Jose Baltazar and Clifford Henderson
School of Chemical and Biomolecular Engineering, Georgia Institute of Technology, Atlanta, Georgia 30332

Samuel Graham[a)]
Electronic Manufacturing and Reliability Laboratory and Woodruff School of Mechanical Engineering, Georgia Institute of Technology, 771 Ferst Drive, Atlanta, Georgia 30332

(Received 27 March 2012; accepted 12 June 2012; published 11 July 2012)

The effect of vacuum annealing followed by exposure to oxygen and water vapor on the unintentional doping of CVD-grown graphene was investigated. CVD graphene samples were cycled between room temperature and 500 °C in vacuum while *in situ* Raman measurements were recorded. During the heating and cooling cycle, a hysteresis in the Raman response due to the desorption of *p*-dopants was observed. Upon exposure to O_2 gas or air, a blue shift in the Raman response with respect to the as grown film was observed which was due to increased adsorption of *p*-dopants on the sample. Experiments showed that a combination of water vapor and oxygen is more effective in *p*-doping the samples than just oxygen and that the doping effects are reversible in both cases. Electrical measurements performed on back-gated field effect graphene devices indicate that shifts in the Dirac point correlate well to the shifts in the Raman peak positions as well as changes found in XPS and Kelvin Probe measurements, verifying the changes in doping of the graphene. © *2012 American Vacuum Society*. [http://dx.doi.org/10.1116/1.4731472]

I. INTRODUCTION

The development of CVD graphene[1,2] is of technological importance as it readily enables large area films from which transparent electrodes, transistors, and other electronic devices can be developed.[3–5] However, CVD graphene requires the removal from its metal growth substrate for integration into components and devices. This process often involves exposure of the graphene to a range of aqueous solutions as well as the atmospheric gas environment,[6] resulting in a host of chemical groups that are attached to the graphene once it is transferred to the target substrate. The impact of these chemical species on single layer graphene is of significant importance in controlling the electronic properties as molecules adsorbed on the surface may change the level and nature of doping in the graphene and is often not the intent of the process (referred to as unintentional doping).[7] Previous research has shown that the doping level in graphene can be modified through adsorption or desorption of gas/vapor molecules (e.g., H_2O, CO, NH_3, etc.).[8] This effect has been explored in order to develop graphene for environmental and biological sensor applications.[9–13] Other examples of such graphene-based devices include ultrafast sensors made using positively gated reduced graphene oxide field effect transistors (FETs)[14] and low cost, miniaturized graphene *p*H sensors.[15]

Thermal annealing has been investigated as a method to change the interaction of graphene with adsorbed molecules from the environment thereby affecting its electrical properties.[16–20] However, it is still unclear as to the mechanisms or functional groups which are responsible for the unintentional doping in graphene, and how the attachment of the functional groups correlates to shifts in the *p*-doping level and charge mobility of graphene. Therefore, additional work is needed to better understand this environmentally induced unintentional doping effect and the degree to which it can be controlled or manipulated.

Here, we present a study of the effects of vacuum annealing and the subsequent exposure of CVD graphene to controlled environmental conditions on its unintentional doping levels. CVD graphene films were grown on copper foils and subsequently transferred onto insulating substrates. The graphene films were characterized in an environmental chamber using *in situ* Raman spectroscopy and *ex situ* x-ray photoelectron spectroscopy, Kelvin probe measurements, and using back gated field effect transistor structures before and after annealing. The results indicate that the vacuum annealing process alters the concentration of adsorbed/desorbed molecules on the CVD graphene, as expected. However, this desorption process leaves active sites for oxygen and water vapor molecules from the environment to be re-absorbed on graphene resulting in a more highly *p*-doped film. The complexity of the process shows the importance of the thermal and environmental history on the unintentional doping of graphene films.

II. EXPERIMENT

Graphene was grown on 25 μm Cu foils using a low pressure chemical vapor deposition technique.[5] The Cu substrates were heated up to 1000 °C in a low pressure Ar/H_2 environment and were annealed for 30 min to increase the

[a)]Author to whom correspondence should be addressed; electronic mail: sgraham@gatech.edu

Cu grain size. In a typical growth step, CH_4 was introduced for 15 min, and the sample was cooled to room temperature rapidly maintaining the same gas flow. The graphene samples were transferred onto SiO_2 substrates while care was taken to minimize the introduction of defects during the transfer process.[5] During the transfer process, the Cu was etched in iron chloride (30%) overnight and graphene samples were treated with hydrochloric acid (10%) for 10 min, followed by washing in deionized water to remove contaminants on the graphene film.[21]

After their transfer onto the SiO_2 substrate, Raman spectroscopy was utilized to investigate the quality of the as-grown graphene on Cu by examining the *D*, *G*, and 2D bands. All spectra were excited with visible (532 nm) laser light and collected in the backscattering configuration with a laser power below 0.5 mW to avoid laser-induced heating.[16] A 50x objective lens was used to focus the laser on the graphene samples during the Raman measurements. The samples were placed inside an environmentally controlled microscope stage with heating, vacuum, and gas delivery capability (Linkam TS 1500) for *in situ* Raman measurements. The thermal stage was mounted onto an X-Y-Z micropositioning stage to control focusing and the measurement position. A quartz window was used to allow optical access to the sample while a vacuum pump was used to evacuate the pressure down to 1 mTorr. The temperature was controlled between room temperature and 500 °C. The drift of the laser spot on the graphene due to thermal expansion was minimized before all measurements. The sample was heated up to each set point temperature and held for 15 min to ensure temperature stability and to allow for desorption of surface functional groups bonded to the sample. Raman measurements were performed at each temperature set point both on heat up and cool down at several different spots on the surface of the graphene to verify reproducibility. After cool down, the sample was exposed to N_2, O_2, and air while Raman measurements were repeated on the same measurement locations using the micropositioning stage. All Raman peaks were fitted with Gauss-Lorentzian line shapes to determine the peak position, linewidth, and intensity of the *D*, *G*, and 2D Raman peaks. A Thermo K-Alpha x-ray photoelectron spectroscopy system was also utilized to determine the elemental composition of the graphene and chemical bonding state before and after annealing and re-exposure to air as well. The transferred graphene films were also fabricated into back-gated field effect transistors with Au/Cr contacts to test the mobility, doping level, and observe the position of the Dirac neutrality point. Highly *p*-doped Si was used as the gate and a 300 nm of thermally grown oxide as the gate dielectric. Finally, a Besocke Delta Phi Kelvin Probe system was used to evaluate the work function of the graphene before and after vacuum annealing and re-exposure to air.

III. RESULTS AND DISCUSSION

Figures 1(a) and 1(b) show the graphitic peak position measured under controlled environmental conditions. Red and blue data indicate the measurement results during the heat up and cool down process of each graphene film, respectively. The *G* and 2D peak positions shifted to lower wave numbers as the temperature increased as previously observed.[22,23] This is partially attributed to both a temperature effect and thermal expansion of graphene at high temperatures. The intrinsic temperature effect depends on anharmonic potential constant as well as phonon occupation number. As the Debye temperature of carbon materials is ~2800 K, the anharmonic contribution can be ignored.[16] Therefore, direct coupling of the phonon modes and thermal expansion induced volume change both contribute to the resulting temperature dependence of Raman spectra. In addition, vacuum annealing at elevated temperature can cause desorption of oxygen groups and moisture which results in de-doping of graphene. A decrease in Raman graphitic peak position due to the de-doping process may also occur. A sudden drop in *G* and 2D peak position measured after vacuum annealing at 100 °C is indicative of possible evaporation of moisture of the substrate. A hysteresis effect observed in *G* and 2D peak positions measured during heat up and cool down process confirm that the desorption of oxygen groups and moisture during vacuum annealing has some impact on the Raman peak position. This is in contrast with previously observed temperature dependence of exfoliated graphene[16,23,24] where *G* and 2D peaks showed a red shift of

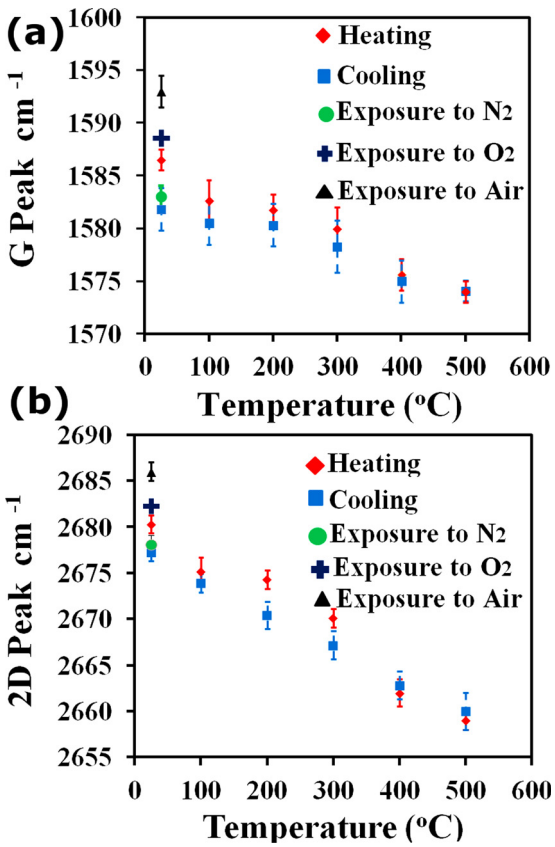

FIG. 1. (Color online) (a) Temperature dependence of *G* peak with ~12 cm^{-1} blue shift due to vacuum annealing and re-exposure to air. (b) Temperature dependence of 2D peak with ~9 cm^{-1} blue shift due to vacuum annealing and re-exposure to air.

$\sim 5\,cm^{-1}$ and $\sim 3\,cm^{-1}$ due to vacuum annealing, respectively. Temperature coefficient for the shift in the *G* and 2D bands in CVD-grown graphene was measured as $0.024\,cm^{-1}\,°C^{-1}$and $0.044\,cm^{-1}\,°C^{-1}$, respectively. This indicates the higher sensitivity of the 2D peak to temperature change as the 2D peak is a second-order phonon peak and the shift is enhanced for the second harmonic.[25]

After vacuum annealing and cool down, the sample was exposed to N_2 gas in the Linkham stage and the Raman measurements were repeated after 30 min as a control. The peak positions did not experience a significant change as expected. Next, O_2 was introduced inside of the Linkham stage and the samples were exposed from 5–60 min. *In situ* Raman measurements showed a significant increase in the *G* and 2D peak positions. It is important to note that a saturation in the oxygen adsorption was observed as further increase in exposure to O_2 gas did not result in an additional shift in the peak position.[19] Following oxygen exposure, the sample exposed to air resulting in a further increase in the Raman peak positions indicative of additional doping through the adsorption of water vapor to the edges and defect sites of the graphene.[16] Figure 1(a) shows the blue shift in the *G* peak position up to $\sim 12\,cm^{-1}$, which is in accordance with other reported doping effects by air exposure.[25,26] The 2D peak position is known to increase with hole doping and decreases with electron doping.[25] In our analysis, the 2D peak position shifted $\sim 9\,cm^{-1}$ through O_2 exposure followed by air exposure. The observed shift in the 2D peak position induced by atmospheric *p*-dopants is similar to the one that reported after graphene *p*-doping by electrostatic gating.[16,25] It is important to note that this vacuum annealing and re-exposure to air process does not induce defects to the structure of the graphene. Raman spectra of graphene after undergoing vacuum annealing, cooling, and air/gas exposure cycles show no detectable defect peaks as shown in the supplementary material Fig. S1.[27]

Since it is believed that the oxygen containing groups responsible for the *p*-doping are physisorbed to the graphene, their attachment and detachment may be reversible depending on changes in the environmental conditions. To explore this, another set of measurements was performed to investigate the reversibility of the doping process through O_2 gas and air exposure. Figure 2(a) shows the *in situ* Raman *G* peak position of graphene samples having undergone various annealing and gas/air exposure steps. First, sample #1 was placed inside of the Linkham stage and heated in vacuum to 500 °C, resulting in a decrease in *G* peak position from $1587\,cm^{-1}$ down to $1574\,cm^{-1}$. Upon cooling to room temperature, the peak position increased, but remained at a reduced value of $1581\,cm^{-1}$ corresponding to the de-doping of the graphene film. Next, a N_2 exposure resulted in no significant change in the Raman peak position. After the N_2 exposure, a 5 min O_2 exposure resulted in a significant shift in the *G* peak position to $1585\,cm^{-1}$ while further exposure from 30–60 min caused a slight change to $1587\,cm^{-1}$. This indicates that the O_2 adsorption is a fast process and saturates before an hour exposure.[19] Re-exposure of the sample to N_2 environment for 30 min resulted in a decrease in the peak position back to $1581\,cm^{-1}$ showing the reversibility of the doping process by O_2 adsorption. Subsequent exposure to oxygen resulted in the *G* peak shifting back to its saturated O_2 doped position of $1587\,cm^{-1}$. This is in accordance with the reversibility of doping with dry O_2 reported for exfoliated graphene.[19] Subsequent exposure to air resulted in a significant increase in the *G* peak position to $1594\,cm^{-1}$ as shown in Fig. 2(a). In Fig. 2(b) sample #2 was subjected to a similar heating and cooling cycle, but exposed to air directly rather than having an intermediate O_2 exposure step. As expected, a significant blue shift was observed in Raman *G* peak position, increasing from $1581\,cm^{-1}$ after vacuum annealing to $1594\,cm^{-1}$. However, in contrast to doping with

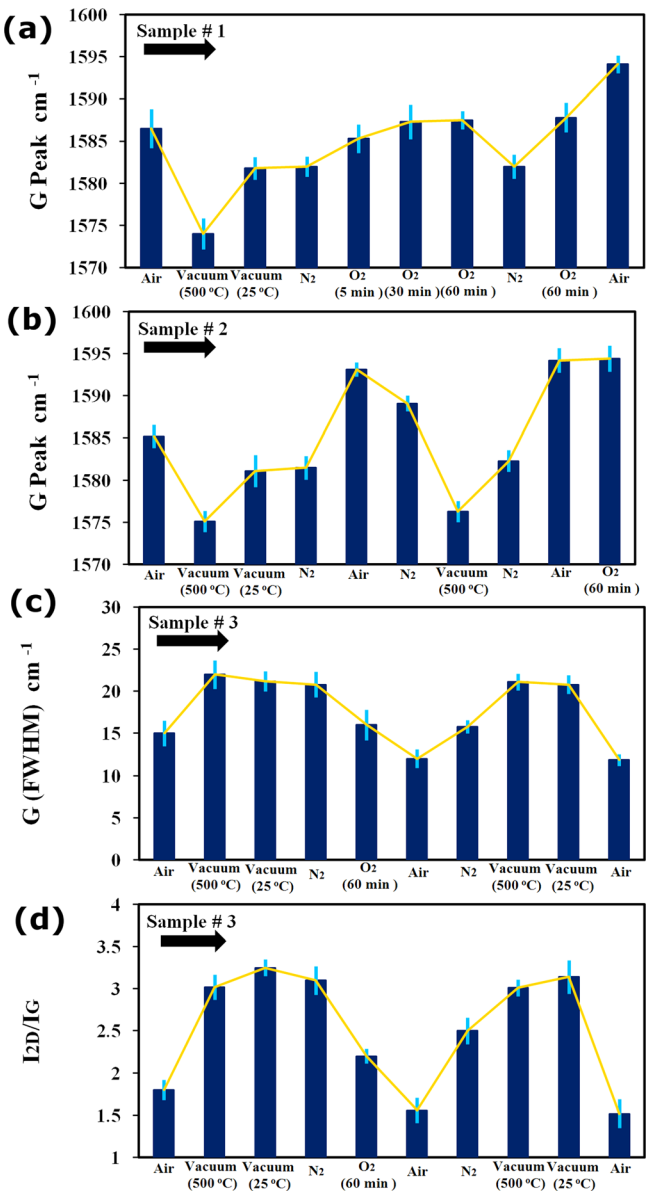

FIG. 2. (Color online) Oxygen and water vapor doping reversibility study. (a) Variation in *G* peak position of sample #1 as it undergoes annealing and gas/air exposure steps. (a) Variation in *G* peak position of sample #2 as it undergoes annealing and gas/air exposure steps. (c) Variation in FWHM (*G*) peak of sample #3 as it undergoes annealing and gas/air exposure steps. (d) Variation in FWHM (*G*) peak of sample #3 as it undergoes annealing and gas/air exposure steps.

dry O_2, exposure of the sample to a N_2 environment did not shift the peak position back to its initial position of 1581 cm^{-1}, but 1589 cm^{-1}. It should be noted that the sample exposed to air can be doped by water vapor as well as O_2 and other oxygen containing molecules. The decrease in the doping level during the exposure to dry N_2 may be a result of the removal of molecules such as O_2 that are weakly absorbed to the graphene. However, other molecules such as water have much stronger bonds to the graphene and do not readily desorb in the dry N_2 environment. Next, the sample was vacuum annealed in the Linkham stage up to 500 °C to determine if the adsorbed molecules could be removed. The data show that after heating to 500 °C and cooling back to room temperature, the Raman peak position returned to 1581 cm^{-1}. Again, another exposure to air resulted in an increase in the Raman peak position to 1594 cm^{-1} demonstrating the reversibility of the process. Additional O_2 gas followed by air-exposure did not result in a significant shift in the peak position.

Figures 2(c) and 2(d) illustrate the variation of FWHM of the G peak and intensity ratio of 2D to G peak (I_{2D}/I_G) of sample #3 before and after vacuum annealing and controlled exposure to different gas/air environments. The significant difference of intensity ratio while heating and cooling is an indication of a change in the electronic structure of CVD graphene due to annealing in vacuum and before exposure to air. A sharpening of ~3 cm^{-1} in G peak with 0.5 decrease in the I_{2D}/I_G ratio was observed. The change in the FWHM of the G peak and I_{2D}/I_G ratio for both samples having undergone N_2, O_2, and air exposure cycles is consistent with the shift in the G and 2D peak position indicative of de-doping and p-doping processes. However, FWHM of the G peak experienced a temperature dependence which is in contrast with the previous report.[23]

To investigate the effect of the thermal annealing of CVD graphene and re-exposure to air on its chemical composition, x-ray photoelectron spectroscopy was utilized. XPS data were acquired using a spectrophotometer (VG Scientific ESCALAB 210) with an Al Kα x-ray source ($h\upsilon = 1486.68$ eV). Each surface was examined over a minimum of at least three spots. XPS measurements were first conducted on a SiO_2 substrate that had been taken through the same graphene transfer process. This initial test was designed to determine the baseline of any residual elements and chemical groups on the substrate. Next, CVD graphene films transferred onto SiO_2 substrates were measured before as well as after vacuum annealing followed by re-exposure to air. The survey scan spectra were collected over the binding energy (BE) range of 0–1100 eV with a step size of 1 eV at a pass energy of 200 eV and a spot size of 400 μm. This scan showed the most prominent peaks to be C1s and O1s. Oxygen was abundant on the surface, as the graphene had been transferred to a substrate of SiO_2. Consequently, it was not easy to detect changes in the oxygen peak in samples that were evaluated before and after the heat treatment. Therefore, only high resolution XPS spectra of C1s BE acquired over 282–293 eV with 400 μm spot size, 0.1 eV step size, and 50 eV pass energy (in Fig. 3) were used for analysis. Thermo Avantage v4.54 Build 02750 software was utilized for the analysis of the collected spectra where a Shirley-type background was subtracted and 70% Gaussian-30% Lorentzian curve fitting was performed. The O1s BE was utilized for calibration purpose through charge shifting the O1s peak from SiO_2 to BE of 533 eV.[28] The O1s BE before and after vacuum annealing and re-exposure to air is given in the supplementary material Fig. S2.[27] In order to deconvolute the C1s peak, its BE was set at 284.6 eV, and the peak-fitting procedure was repeated until an acceptable peak was obtained. A line shape analysis revealed four main components centered at binding energies of 284.6, 285.4, 286.1, and 287.8 eV. In agreement with results published elsewhere,[29] the peak at 284.6 eV is assigned to the C-C (sp^2), while the 285.4, 286.1, and 287.8 eV are attributed to defect (sp^3), C-OH, and C=O, respectively. These peaks verify the presence of surface functional groups on CVD graphene due to the process it undergoes in growth and transferring onto insulator substrates. The atomic concentration of different peaks assigned to C1s was compared before and after vacuum annealing followed by exposure to air (see Table I). Hydroxyl (-OH) and carbonyl (C=O) groups are the most dominant groups that decrease after vacuum annealing and re-exposure to air. This decrease provides more room for oxygen and water vapor to be adsorbed on graphene upon exposure to dry gas or air and that results in an additional p-doping of graphene. The energy position of the C1s core level peak shifts as indicated by the dashed line in Fig. 3 which is in accordance with previous reports of graphene p-doping through chemical treatment.[29] As explained earlier, oxygen and water vapor are well-known electron acceptors.

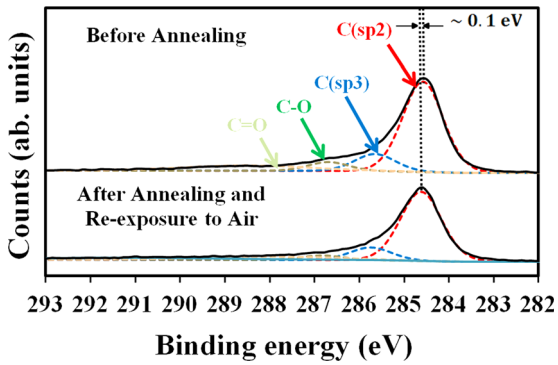

FIG. 3. (Color online) Core-level x-ray photoelectron spectroscopy (XPS) peaks showing typical shift and broadening caused by vacuum annealing and exposure to air.

TABLE I. (Top) Work function changes with vacuum annealing and exposure to air measured by Kelvin Probe. (Bottom) Atomic % of different peaks assigned to C1s before and after vacuum annealing followed by exposure to air.

		Before annealing 5.0 ± 0.05	After annealing 5.2 ± 0.05
Work function		At. %	At. %
XPS	C (sp^2) 284.6 eV	61.2	68.5
	C (sp^3) 285.4 eV	12.5	14
	C-OH 286.1 eV	14.1	5.7
	C=O 287.8 eV	12.2	11.8

Therefore, adsorption of these species on graphene makes electron ejection more difficult, which translates to a higher C1*s* BE Table I summarize those changes in the atomic percentages before and after annealing and re-exposure to air.

To further investigate the *p*-doping in graphene due to annealing followed by air exposure and to corroborate the results of XPS and Raman spectroscopy measurements, electrical characterization using field effect transistors was performed. A back-gated FET was fabricated by transferring CVD graphene onto heavily doped Si with a 300 nm thick thermal oxide layer followed by lithography, plasma etching, and Cr/Au metallization with a FET channel size of 50 μm wide and 2 mm length. The image of the device is shown in Fig. 4(a). Figure 4(b) shows source-drain current (I_{DS}) versus gate voltage (V_g) of a graphene-based FET device as transferred and then after annealing and re-exposure to air. A positive neutrality point voltage (V_{NP}) on the order of 20 V demonstrates *p*-doped characteristics, which are attributed to chemical groups bounded to graphene due the transfer process. The electron and hole mobility for the as-made device is $\sim 108 \pm 50$ cm^2/Vs and $\sim 217 \pm 50$ cm^2/Vs. Annealing at 200 °C results in a decrease in V_{NP} close to zero and an increase in electron and hole mobility up to $\sim 217 \pm 50$ cm^2/Vs and $\sim 434 \pm 50$ cm^2/Vs, respectively. This is due to the removal of *p*-dopants by annealing that leads to pristine graphene with higher mobilities. After annealing and re-exposure to air, an increase in the V_{NP} higher than 60 V observed. This confirms an increase in accumulation of *p*-dopants due to annealing and re-exposure to air. A dopant concentration of 1×10^{13} cm^{-2} was calculated for the device after annealing and re-exposure to air with a hole mobility 65 ± 35 cm^2/Vs. Figure 4(c) shows the I_{DS} vs V_g measured on the same sample after being annealed. An increase in annealing time and temperature showed a decrease in V_{NP} corresponding to the de-doping process. This confirms the removal of *p*-dopants due to annealing as the V_{NP} shifted to zero voltage after 3 h annealing indicative of very little doping in the graphene sample. The stability and reversibility of atmospheric doping were also investigated. To this end, the annealed sample at 200 °C for 3 h exposed to air for 1 h. V_{NP} is shifted from zero to more than 10 V indicative of *p*-doping and electron and hole mobility decreased to the order of $\sim 130 \pm 50$ cm^2/Vs and $\sim 220 \pm 50$ cm^2/Vs, respectively. The sample underwent the same heat treatment cycle and as a result V_{NP} shifted back to zero and electron and hole mobility shifted back to their initial values. ($\sim 217 \pm 50$ cm^2/Vs for electrons and $\sim 434 \pm 50$ cm^2/Vs for holes.) However, an inert N_2 environment resulted in no change in the V_{NP}. The observed atmospheric doping effect reversible by heat treatment and irreversible by N_2 environment is consistent with the Raman measurements.

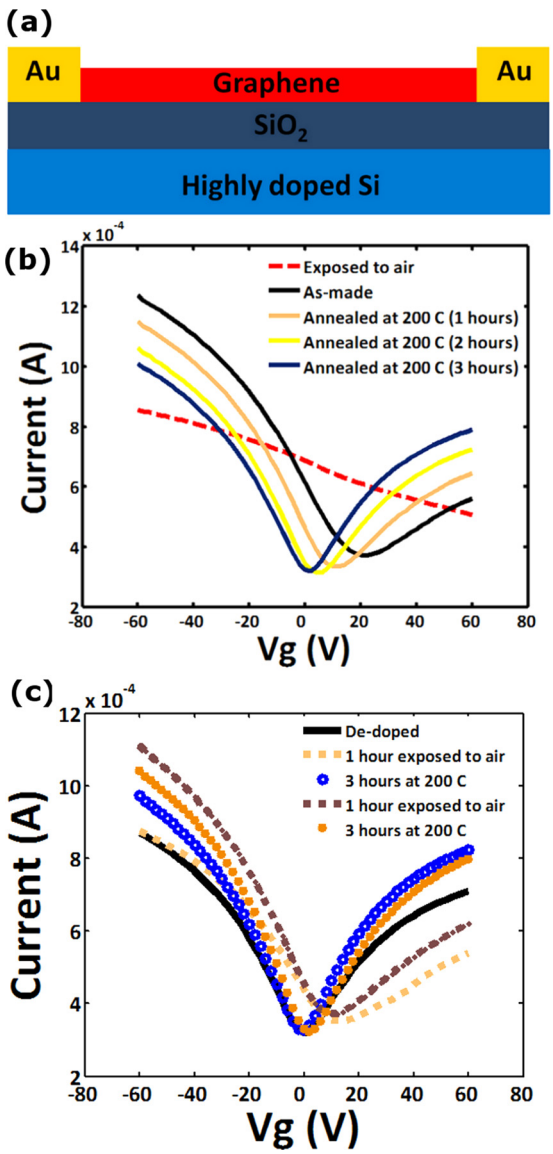

FIG. 4. (Color online) (a) IV curve showing *p*-doping of graphene after annealing and re-exposure to air. (b) De-doping of graphene due to heating in vacuum over time. Inset: Schematic of device (stack).

The work function of graphene before and after vacuum annealing and environmental exposure was measured by Scanning Kelvin Probe (Besocke Delta Phi).[30,31] Kelvin Probe work function measurements were averaged over three locations on each substrate. A highly ordered pyrolytic graphite sample with a work function of 4.5 eV was used as the reference sample. The measurement results are shown in Table I. The work function measured on as-transferred CVD graphene was ~5 eV which is higher than pristine graphene, ~4.7 eV, indicative of intrinsically *p*-doped sample. Kelvin probe measurements were repeated on transferred CVD graphene after vacuum annealing and re-exposure to air. An increase in the work function after annealing and re-exposure to air up to 0.2 eV was observed indicative of further adsorption of atmospheric *p*-dopants. A higher annealing temperature results in heavier *p*-doping, which translates to more shift in the Fermi energy level. This increase is considered to provide direct evidence for chemical/molecular desorption/adsorption of O_2, H_2O, and chemical groups on the graphene surface.

IV. CONCLUSIONS

We demonstrate that a change in the oxygen containing groups on the graphene film induced by both annealing and

re-exposure to air results in a *p*-doping on graphene samples. The shift in the Raman graphitic peak positions and neutrality point of FET device made of graphene before and after annealing confirms this change. XPS measurements revealed the change in chemical species on graphene, resulting in a *p*-doping. The change in the Fermi energy level was confirmed by work function measurements before and after annealing and exposure to air. The ability to use vacuum annealing to systematically tailor the surface potential of CVD graphene makes it a potential material for device applications.

ACKNOWLEDGMENTS

The authors wish to acknowledge Bernard Kippelen and Yinhua Zhou for work function measurement. The authors thank Walter Henderson for fruitful discussions on XPS data. This work is supported by Georgia Tech MRSEC and National Science Foundation, Grant No. 0927736.

[1]K. S. Novoselov, A. K. Geim, S. V. Morozov, D. Jiang, Y. Zhang, S. V. Dubonos, I. V. Grigorieva, and A. A. Firsov, Science **306**, 666 (2004).
[2]C. Berger *et al*., Science **312**, 1191 (2006).
[3]Q. K. Yu, J. Lian, S. Siriponglert, H. Li, Y. P. Chen, and S. S. Pei, Appl. Phys. Lett. **93**, 113103 (2008).
[4]K. S. Kim, Y. Zhao, H. Jang, S. Y. Lee, J. M. Kim, J. H. Ahn, P. Kim, J. Y. Choi, and B. H. Hong, Nature **457**, 706 (2009).
[5]X. S. Li *et al*., Science **324**, 1312 (2009).
[6]M. P. Levendorf, C. S. Ruiz-Vargas, S. Garg, and J. Park, Nano Lett. **9**, 4479 (2009).
[7]L. Liu, S. Ryu, M. R. Tomasik, E. Stolyarova, N. Jung, M. S. Hybertsen, M. L. Steigerwald, L. E. Brus, and G. W. Flynn, Nano Lett. **8**, 1965 (2008).
[8]F. Schedin, A. K. Geim, S. V. Morozov, E. W. Hill, P. Blake, M. I. Katsnelson, and K. S. Novoselov, Nature Mater. **6**, 652 (2007).
[9]J. T. Robinson, F. K. Perkins, E. S. Snow, Z. Wei, and P. E. Sheehan, Nano Lett. **8**, 3137 (2008).
[10]J. D. Fowler, M. J. Allen, V. C. Tung, Y. Yang, R. B. Kaner, and B. H. Weiller, ACS Nano **3**, 301 (2009).
[11]A. Ghosh, D. J. Late, L. S. Panchakarla, A. Govindaraj, and C. N. R. Rao, J. Exp. Nanosci. **4**, 313 (2009).
[12]S. Stankovich, D. A. Dikin, G. H. B. Dommett, K. M. Kohlhaas, E. J. Zimney, E. A. Stach, R. D. Piner, S. T. Nguyen, and R. S. Ruoff, Nature **442**, 282 (2006).
[13]Y. Dan, Y. Lu, N. J. Kybert, Z. Luo, and A. T. C. Johnson, Nano Lett. **9**, 1472 (2009).
[14]G. H. Lu, K. H. Yu, L. E. Ocola, and J. H. Chen, Chem. Commun. **47**, 7761 (2011).
[15]N. Lei, P. F. Li, W. Xue, and J. Xu, Meas. Sci. Technol. **22**, 107002 (2011).
[16]Z. H. Ni, H. M. Wang, Z. Q. Luo, Y. Y. Wang, T. Yu, Y. H. Wu, and Z. X. Shen, J. Raman Spectrosc. **41**, 479 (2010).
[17]A. Nourbakhsh *et al*., J. Phys. Chem. C **114**, 6894 (2010).
[18]Z. G. Cheng, Q. Y. Zhou, C. X. Wang, Q. A. Li, C. Wang, and Y. Fang, Nano Lett. **11**, 767 (2011).
[19]S. Ryu, L. Liu, S. Berciaud, Y.-J. Yu, H. Liu, P. Kim, G. W. Flynn, and L. E. Brus, Nano Lett. **10**, 4944 (2010).
[20]Y. Yang and R. Murali, Appl. Phys. Lett. **98**, 093116 (2011).
[21]R. S. Pantelic, J. W. Suk, C. W. Magnuson, J. C. Meyer, P. Wachsmuth, U. Kaiser, R. S. Ruoff, and H. Stahlberg, J. Struct. Biol. **174**, 234 (2011).
[22]I. Calizo, S. Ghosh, W. Bao, F. Miao, C. N. Lau, and A. A. Balandin, Solid State Commun. **149**, 1132 (2009).
[23]I. Calizo, A. A. Balandin, W. Bao, F. Miao, and C. N. Lau, Nano Lett. **7**, 2645 (2007).
[24]I. Calizo, F. Miao, W. Bao, C. N. Lau, and A. A. Balandin, Appl. Phys. Lett. **91**, 071913 (2007).
[25]A. Das *et al*., Nat. Nanotechnol. **3**, 210 (2008).
[26]S. Pisana, M. Lazzeri, C. Casiraghi, K. S. Novoselov, A. K. Geim, A. C. Ferrari, and F. Mauri, Nature Mater. **6**, 198 (2007).
[27]See supplementary material at http://dx.doi.org/10.1116/1.4731472 for Raman spectra and XPS O 1s binding energy of graphene before and after annealing and re-exposure to air.
[28]G. Hollinger, Y. Jugnet, P. Pertosa, and T. M. Duc, Chem. Phys. Lett. **36**, 441 (1975).
[29]S. Bae *et al*., Nat. Nanotechnol. **5**, 574 (2010).
[30]I. D. Baikie, U. Petermann, A. Speakman, B. Lagel, K. M. Dirscherl, and P. J. Estrup, J. Appl. Phys. **88**, 4371 (2000).
[31]Y. H. Zhou *et al*., Science **336**, 327 (2012).